JEF/DOC 276

Evaluation of neutron and photon-production cross sections of natural iron isotopes in the incident-neutron energy range 1-20 MeV

by F. Fabbri, G. Maino, E. Menapace, A. Mengoni
ENEA - Nuclear Data and Codes Laboratory - Bologna.

I. Introduction

Production cross section and spectra of photons emitted in neutron-induced reactions are basic data for radiation shielding analysis and heating estimate in both fission and fusion devisec. Since experimental information over a broad incident-neutron energy range (in the MeV region) and for a large number of nuclides is not easily obtainable owing to the difficulties inherent in measurements of this kind, model calculations have to supply it.

In this context, it is useful to check the reliability of commonly-adopted nuclear model reactions and codes together with suitable parametrization of nuclear structure data (such as giant resonance parameters and nulvear level densities) in predicting gamma-ray production data too, in addition to the well-studied fast neutron cross sections.

From a theoretical point of view, this investigation is of some interest in elucidating the mechanisms underlying nuclear reactions and de-excitation processes induced by fast

neutrons. Moreover, as outlined by Larson, evaluations of photon production cross sections, referring to the 2_1^+ ---> 0_1^+ transition in even-even nuclei in the mass region $A \tilde{=} 50-60$ (comprehensive of most structural materials), make an estimate of neutron total inelastic scattering possible.

In fact, these medium-mass nuclei are observed to decay from excited states mainly through the 2_1^+ state, due to its strong collective character. Thus, the cross section for population of this level approximates the total inelastic one to within a few per cent.

If measurements of total inelastic scattering cross sections are clearly difficult, since they require direct observation of scattered neutrons, activation analyses to obtain charged-particle emission cross sections are impossible when final nuclei in the relevant processes are stable. Therefore, in many cases knowledge of total and elastic scattering cross sections, together with an estimate of the magnitude of total inelastic scattering reaction, can supply reliable information about the unknown (n,p) and (n,alpha) cross sections. Calculations for ^{54}Fe and ^{56}Fe, where experimental data about these processes are available, can supply useful checks of adopted nuclear models and parametrizations.

Finally, discrete gamma-rays emitted in (n,n'xgamma) reactions provide the unique signature of the final nucleus involved in the process and, consequently, information on

the relevant tertiary-reaction cross section, which becomes important for E_n > 10 MeV in the $A \tilde{=} 50$-60 mass region.

An evaluation of neutron cross sections and photon production data for chromium isotopes in the continuum region has been recently carried out at ENEA Nuclear Data Laboratory in BOlogna. An analogous evaluation work for stable iron isotopes is presently undertaken. The adopted formalism and codes to calculate the relevant cross sections and spectra are briefly described in the followinf sections. Finally, some results for ^{54}Fe and ^{56}Fe are shown and discussed.

II. Optical model calculations

The spherical-optical-model (OM) parameters deduced by the Los Alamos group have been adopted in the calculation of total and shape-elastic scattering cross section; the geometrical parameters of the real part of the OM potential have been slightly varied in order to reproduce the experimental data above $E_n \tilde{=} 10$ MeV at best as far as charged-particle emission channels are also concerned.

The calculated cross sections and s- and p-wave neutron strength functions agree fairly well with the corresponding measured quantities at $E_n \lesssim 1$MeV.

The deduced OM transmission coefficients have been then introduced in the usual Hauser-Feshbach formalism, to obtain compound-nucleus formation cross sections for all open-channel reactions in the considered incident-neutron energy range ($E_n \lesssim 20$ MeV). Statistical fluctuations have been accounted for in all the reaction channels up to $E_n = 3$ MeV.

III Preequilibrium contributions

Preequilibrium contributions have to be included in addition to usual statistical cross sections in the higher incident-neutron energy region ($E_n \gtrsim 10$ MeV). This has been carried out for neutron, proton and alpha emission channels. Our version of the PENELOPE code, written by Fabbri and Reffo, which has been extensively used for statistical model calculations in the present evaluation, has been slightly modified in order to take into account these preeequilibrium components.

For sake of semplicity, we have considered the naive exciton model without angular momentum conservation, since we are mainly concerned with photon production data which are are less sensitive than emitted-particle spectra to the realistic and improved details of the adopted preequilibrium model.

Therefore, preequilibrium contributions to be added to the statistical cross sections and spectra are simply given by the following formulae in our approach:

$$\frac{d\sigma^{(pe)}_{\alpha,\beta}}{dE_\beta} = \sigma_\alpha(E_\alpha) \sum_{\substack{n=n_0 \\ (\Delta n=2)}}^{\bar{n}} W_\beta(n, E, E_\beta)\, T(n, E) \quad ;$$

$$\sigma^{(pe)}_{\alpha,\beta} = \int_0^{E_{max}} \frac{d\sigma^{(pe)}_{\alpha,\beta}}{dE_\beta}\, dE_\beta \quad ; \qquad E_{max} = E_\alpha + B_\alpha - B_\beta \ ,$$

where the indices α and β refer to the incident neutron and the emitted particle, respectively. E_α is the kinetic energy of the incident neutron and E_β of the emitted particle, while E is the excitation energy of the nucleus. As usual, is the cross section for compound-nucleus formation. Moreover,

$$W_\beta(n, E, E_\beta) = \frac{(2s_\beta+1)}{\pi^2\hbar^3}\mu_\beta E_\beta \sigma_\beta^{inv}(E_\beta)\frac{\omega(p-p_\beta, h, U, E_H)}{\omega(p, h, E, E_H)} Q_\beta(n),$$

with s_β, μ_β and p_β spin, reduced mass and mass number of the emitted particle, respectively. U is the excitation energy of the residual nucleus, once the beta particle has been emitted;

$\sigma_\beta^{inv}(E_\beta)$ is the compound-nucleus cross section for the inverse process where an incident beta particle is assumed.

$\sigma_\beta^{inv}(E_\beta)$ is obtained by means of optical model calculations with the parameters discussed in the previous section. The energy term, E_H, takes into account the finite depth of the hole-potential.

The particle-hole level densities, ω, as function of both hole- and particle-numbers (h and p, respectively) and excitation energy have been assumed in the form given by Kalbach; the same holds for the Q_β factor which represents a correction factor taking into account differences between neutron and proton excitons.

The fraction of time, T(n,E) with n=p+h, spent by the nuclear system in an excited configuration with n excitons and energy E, is given by:

$$T(n,E) = \tau_n(E) \prod_{\substack{i=n_0 \\ (\Delta i=2)}}^{n-2} \left[\lambda^+(i,E)\tau_i(E)\right] ,$$

$$\left[\tau_n(E)\right]^{-1} = \lambda^+(n,E) + \sum_\delta \int_0^{E_\delta^{max}} W_\delta(n,E,E_\delta)\,dE_\delta ,$$

where the summation is extended to all the open reaction channels.

The strength, $\lambda^+(n,E)$, for transition to more complicated configurations with (n+2) excitons has the following form:

$$\lambda^+(n,E) = \frac{2\pi}{\hbar}|M|^2 \omega_f^+(n,E,E_H) ,$$

where ω_f^+ is the density of final states, deduced by Bétak and Dobeš, and M an average matrix element for nuclear tran-

sitions, whose expression has been derived by Kalbach. Its value is taken as an adjustable parameter.

Finally, once a neutron or a charged-particle has been emitted or the nucleus has achieved statistical equilibrium, the system can further decay from its excited configuration by particle emission or gamma-ray de-excitation cascade. In the latter case, we assume that the pre-equilibrium configurations have the same spin and parity distribution as the corresponding statistical configurations at the same excitation energy.

IV Statistical model calculations and nuclear structure information

As for the choice of nuclear structure ingredients in the statistical calculations performed by means of the PENELOPE code (Fabbri and Reffo, unpublished), we have adopted nuclear level schemes and gamma-decay branching ratios from the recent literature (Nuclear Data Sheets and references quoted therein), supplemented by theoretical estimates.

Nuclear excited states, in addition to neutron and/or charged particle emission, are assumed to decay by means of E1, E2 and M1 electromagnetic transitions both to continuum and discrete levels. Higher multipolarity transitions have been considered only for gamma-decays between discrete levels.

Use has been made of the Brink-Axel hypothesis, so as to relate transmission coefficients for neutron radiative capture to photon absorption in the giant-resonance regions by means of the principle of detailed balance.

The isovector giant dipole resonance has been described by a two-humped Lorentzian shape whose parameters have been fitted to the experimental data on photon absorption and scattering. Further information has been provided by theoretical calculations within the framework of collective models of nuclear structure and energy-weighted sum-rule approaches.

Owing to the lack of detailed experimental data, isoscalar and isovector giant quadrupole resonance parameters have

been deduced from semiclassical and sum-rule estimates; moreover, isovector giant spin resonances, in particular M1, have been completely neglected, since they are likely to be largely fragmented or even suppressed from available measurements.

The cross section for emission of a particular gamma-ray has been then calculated by following the gamma-ray cascade occurring after each inelastic process induced by the incoming neutron. The preequilibrium contributions have also been considered, as outlined in the previous section.

Furthermore, the present statistical calculations allow up to seven successive gamma-ray emissions to reach the ground-state of final nuclei in each exit channel. This limit is high enough for incident-neutron energies less than 20 MeV. In fact, an average photon multiplicity of less than or equal to six was recently measures for both ($n+^{52}Cr$) and ($n+^{56}Fe$) reactions by Oblozinsky and coworkers.

V Nuclear Level Density

The level density of the nuclei involved in the present evaluation were calculated according to the following prescriptions:

1) the available experimental discrete level were used at low excitation energy.

2) A unique formula (see below) were used to reproduce the level density at both low and high excitation energies.

3) The parameters of the adopted models were determined from either experimental information or from a local systematics built up for the present evaluation.

A Fermi-Gas formula were used of type:

$$\rho(U, J, \Pi) = \frac{(2J+1)\, e^{-\frac{J(J+1)}{2\sigma^2}}}{\sigma^2} \quad \frac{e^{2\sqrt{aU}}}{24\,\sigma\sqrt{2}\, a^{1/4} U^{5/4}} \quad F_{par}(U, \Pi)$$

where U is the excitation energy, σ is the spin distribution cut-off parameter and a is the level density parameter related to the single particle level spacing.

The Fermi-Gas formula has been corrected for various effects. Namely:

- odd-even effects

Parity effects can be treated re-defining the excitation energy

$$U' = U - \delta$$

where δ is the pairing energy.

- shell effects

The shell correction to the Fermi-Gas Model can be made taking, as suggested by Igniatyuk, an energy dependent parameter a:

$$a(U) = a(*)[1 + \frac{\delta E_{sh}}{U}(1 - e^{-\gamma U})]$$

where a(*) is the asymptotic or Fermi-Gas value. γ is a parameter that we have taken to have a value of 0.054 MeV^{-1}. δE_{sh} is the shell correction energy calculated as suggested by Igniatyuk from mass-Liquid Drop Model values.

-parity effects

When suggested by microscopic (BCS) calculations that there could be parity effects we have approximated the correction term as

$$F_{par}(U, \Pi) = \begin{cases} 1/2 \ \tanh \frac{\alpha U}{2} & \Pi = -\Pi_c \\ 1 - 1/2 \ \tanh \frac{\alpha U}{2} & \Pi = -\Pi_c \end{cases}$$

where Π_c is the parity of the composite system. The parameter α were determined either by BCS calculations or by the requirement that both the level spacings $\langle D \rangle_{\Pi=0}$ and $\langle D \rangle_{\Pi=1}$ had to be reproduced by the calculations.

Using this approach we have realized that it is possible to fit at the mean time the level density at low excitation energy as well as at the neutron binding if, in addition to the parameter a(*) we also fit a parameter Δ_f to be added to the effective excitation energy :

$$U'' = U' + \Delta_f$$

Therefore, in summary we have fitted *only two parameters*, a(*) and Δ_f, for each nucleus where low-lying levels and level spacing were known and one parameter, Δ_f, for nuclei of unknown level spacing at the neutron binding energy. For the latter, the parameter a(*) were taken from the systematics which is much more reliable once that the corrections described above are applied.

In fig. 1 we show the systematics of both Δ_f and a(*) determined from level spacings *and* low-lying levels fit. As one can see the behaviour of a(*) follows reasonably well the Fermi-Gas result a $\propto$ A. On the othe

hand Δ_f does not show any systematic trend. For the mass region under study we have observed in any case -0.8 MeV $< \Delta_f < 0.8$ MeV.

Figs. 2a, 2b, 2c, 2d, 2e, and 2f show the fit of the comulative number of low-lying levels for all the iron nuclei involved in the present evaluation. As one can see the fit is quit good for all isotopes, confirming the validity of the technique used for the calculations.

The level density parameters used in the calculation are given in Table 1.

VI Results

The calculated cross sections for (n,2n) and (n,p) reactions on ^{54}Fe and ^{56}Fe are shown in figs. 3-6, in comparison with experimental data. Dashed and solid lines refer, respectively, to calculations performed without and with preequilibrium contributions, and different choices for level density parameters.

Finally, figs.7 and 8 present the calculated emitted-neutron spectra in (n,n') inelastic scattering reactions on both ^{54}Fe and ^{56}Fe, respectively. The preequilibrium component (dashed line) has been added to the statistical spectrum (solid line) in both cases.

Level Density Parameters

Mass region 45 < A < 60

Nucleus	a(*) (MeV-1)	gamma (MeV-1)	alfa (MeV-1)	fdelta (*) (MeV)	csig2	sig2(lev)	Ecut (MeV)
46-Ti	(5.250)	0.054	0.20	-0.6898	0.0139	5.2583	
47-Ti	5.467	0.054	0.20	0.5024	0.0139	7.8409	
48-Ti	5.738	0.054	0.20	-1.2853	0.0139	4.6964	
49-Ti	6.148	0.054	0.20	-0.0944	0.0139	7.2692	
50-Ti	6.217	0.054	0.20	-1.9975	0.0139	5.7917	
51-Ti	6.790	0.054	0.20	-0.5587	0.0139	7.9667	
52-Ti							
49-V	(5.750)	0.054	0.40	0.8403	0.0139	7.0714	
50-V	(5.750)	0.054	0.40	1.4105	0.0139	9.0536	
51-V	6.455	0.054	0.40	-0.5750	0.0139	8.2105	
52-V	5.862	0.054	0.40	1.2657	0.0139	6.5536	
53-V	(6.250)	0.054	0.40	0.2702	0.0139	6.7727	
54-V	(6.500)	0.054	0.40	1.1520	0.0139	6.1250	
49-Cr							
50-Cr	(6.000)	0.054	0.40	-0.9089	0.0139	7.2679	
51-Cr	5.582	0.054	0.22	0.7209	0.0139	8.9375	
52-Cr	(6.250)	0.054	0.40	-1.2161	0.0139	9.0662	
53-Cr	6.387	0.054	0.19	-0.1564	0.0139	8.9800	
54-Cr	5.881	0.054	0.40	-0.9692	0.0139	7.0139	
55-Cr	6.529	0.054	0.19	0.0297	0.0139	6.3261	
53-Mn	(6.250)	0.054	0.40	0.4055	0.0139	9.7581	
54-Mn	(6.250)	0.054	0.40	1.4318	0.0139	8.1250	
55-Mn	(6.500)	0.054	0.40	0.2425	0.0139	6.5192	
56-Mn	6.604	0.054	0.40	1.5288	0.0139	7.1685	
57-Mn	(6.750)	0.054	0.40	0.3875	0.0139	7.5833	
58-Mn	(6.850)	0.054	0.40	1.4444	0.0139	6.1250	
52-Fe							
53-Fe	(6.250)	0.054	0.20	0.4612	0.0139	8.9130	3.470
54-Fe	(6.250)	0.054	0.40	-1.0519	0.0139	6.6875	3.300
55-Fe	6.728	0.054	0.20	0.2832	0.0139	8.6750	3.080
56-Fe	(6.750)	0.054	0.40	-1.0518	0.0139	5.6402	4.520
57-Fe	6.691	0.054	0.20	0.3700	0.0139	4.6875	2.120
58-Fe	6.277	0.054	0.20	-0.5542	0.0139	6.8472	
59-Fe	7.114	0.054	0.20	0.1138	0.0139	4.5476	

Table 1

(*) fdelta $\equiv \Delta_4 - \delta$

References

E.Betak and J.Dobeš, Z.Phys. A297 (1976) 319.

A.V. Ignatyuk et al., Sov. J. Nucl. Phys. 21 (1975) 21;

C.Kalbach, in Proceed. of IAEA Advisory Group Meeting on Basic and Applied Problems of Nuclear Level Densities, report BNL-NCS-51694 (1983), p.113.

D.C.Larson, Radiat. Eff. 95 (1986) 71.

Los Alamos, 8626-MS (ENDF-304), 1980.

A.Mengoni, F.Fabbri and G.Maino, Nuovo Cim. 94A (1986) 297 ; ENEA report RT/TIB/85/38, Rome (1985).

P.Oblozinsky, in IAEA report INDC(NDS)-173/GI, Vienna (1985), p.62.

P.Oblozinsky and S.Hlavac, IAEA report INDC(CSR)-6/GI, Vienna (1985), p.17.

Fig. 1

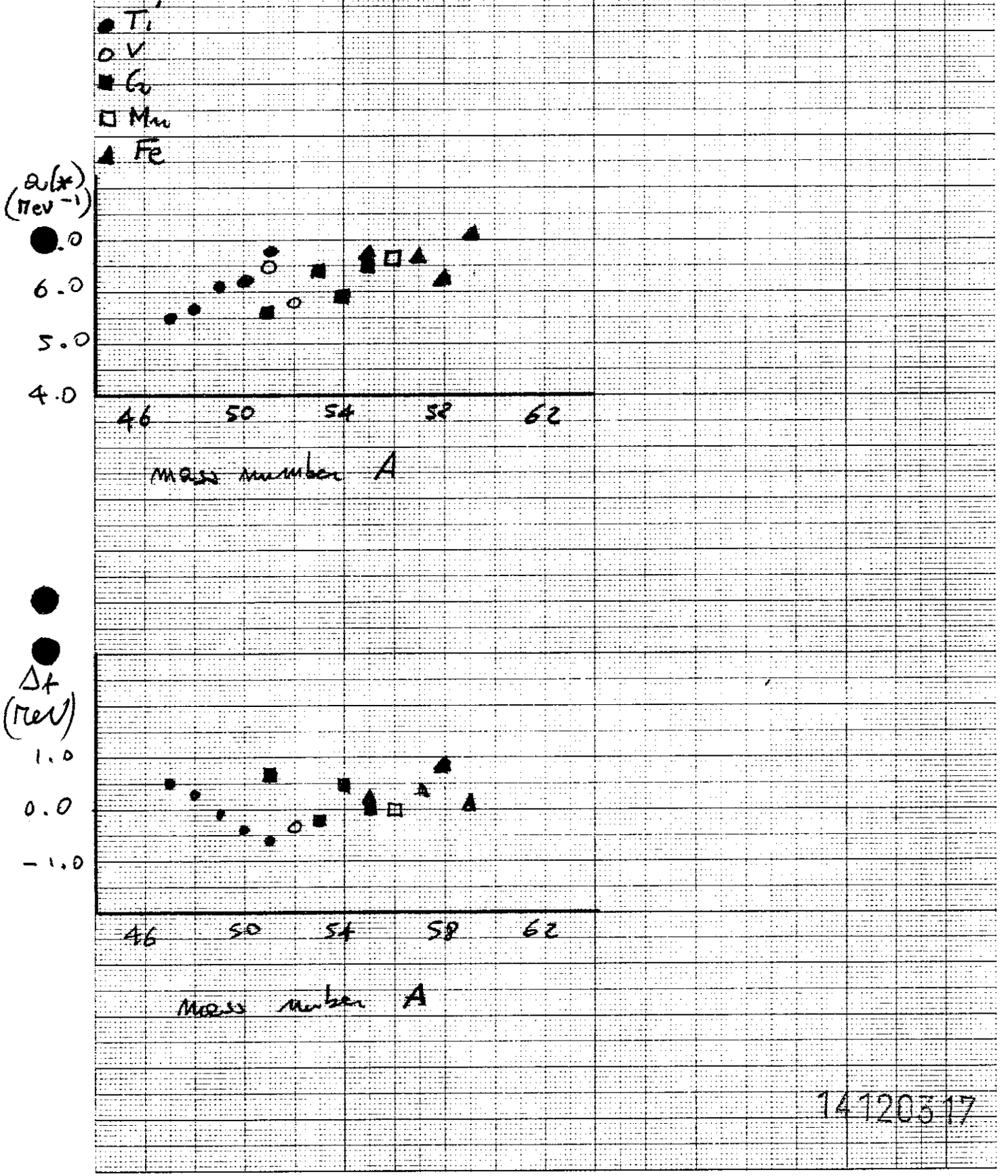

1412017

Fig. 25

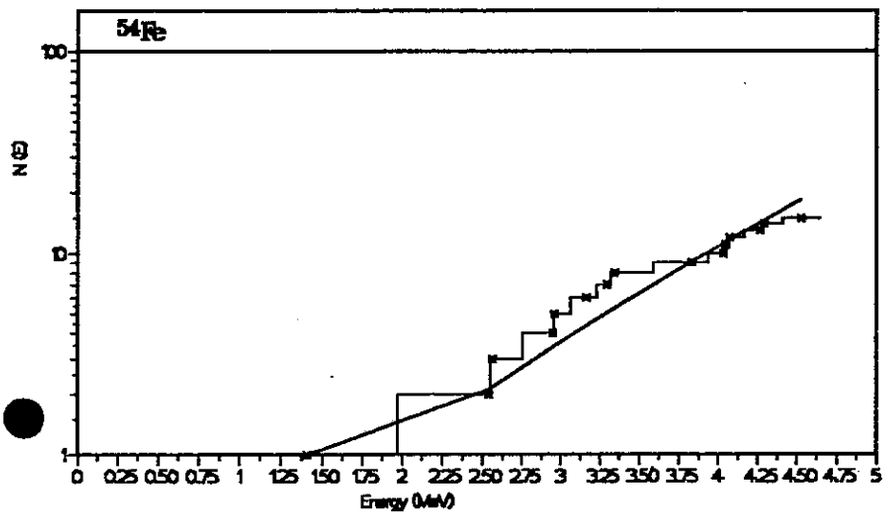

Fig. 26

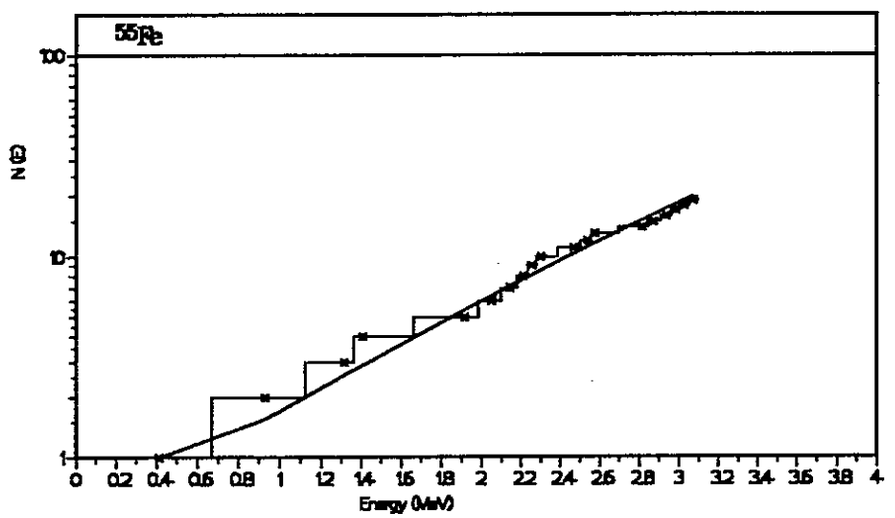

Fig. 2c

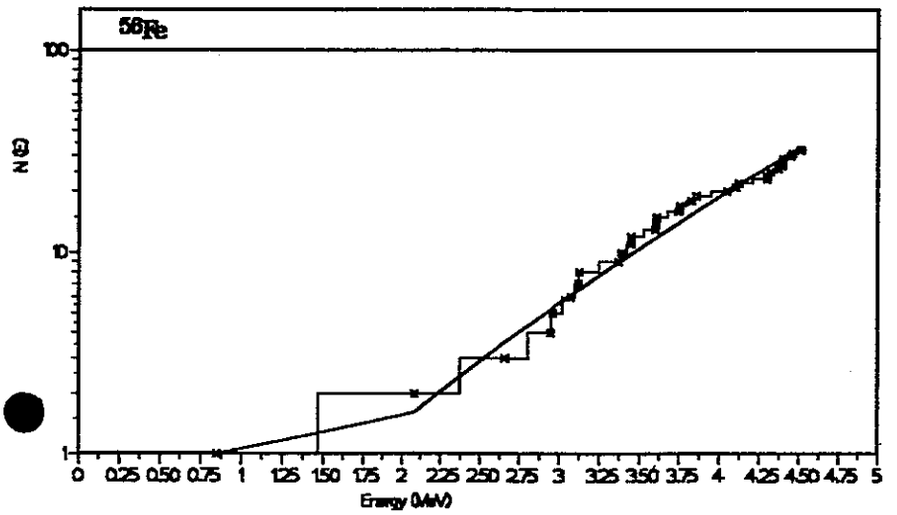

Fig. 2d

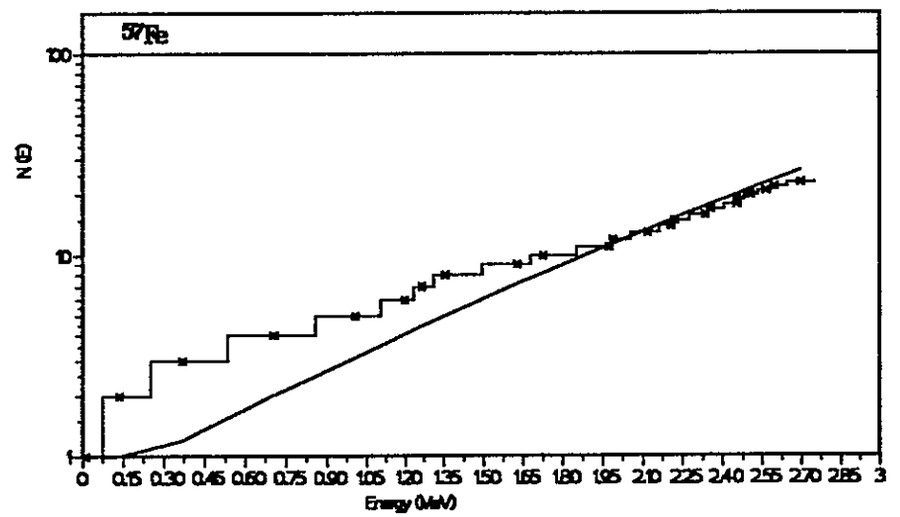

Fig. 2e

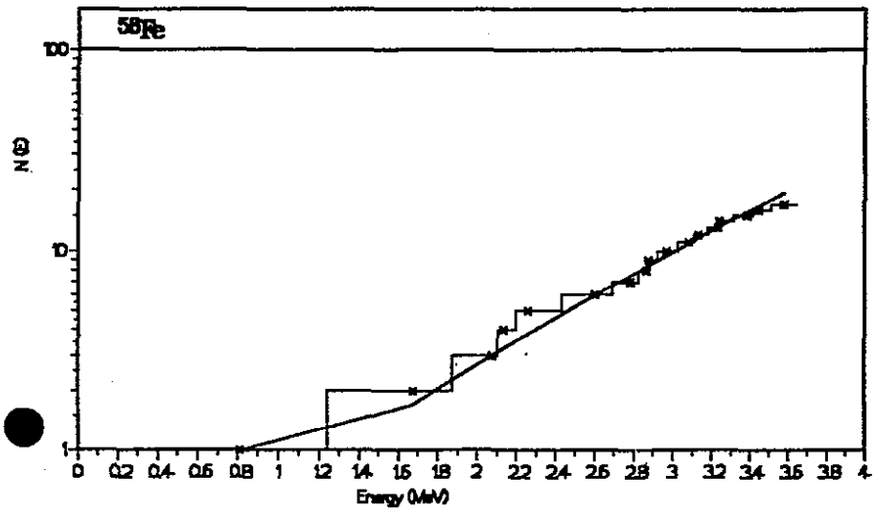

Fig. 2f

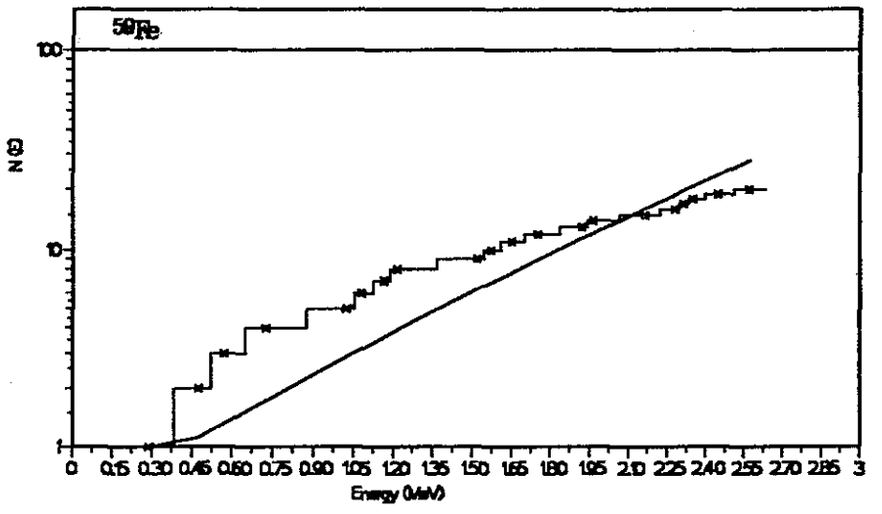

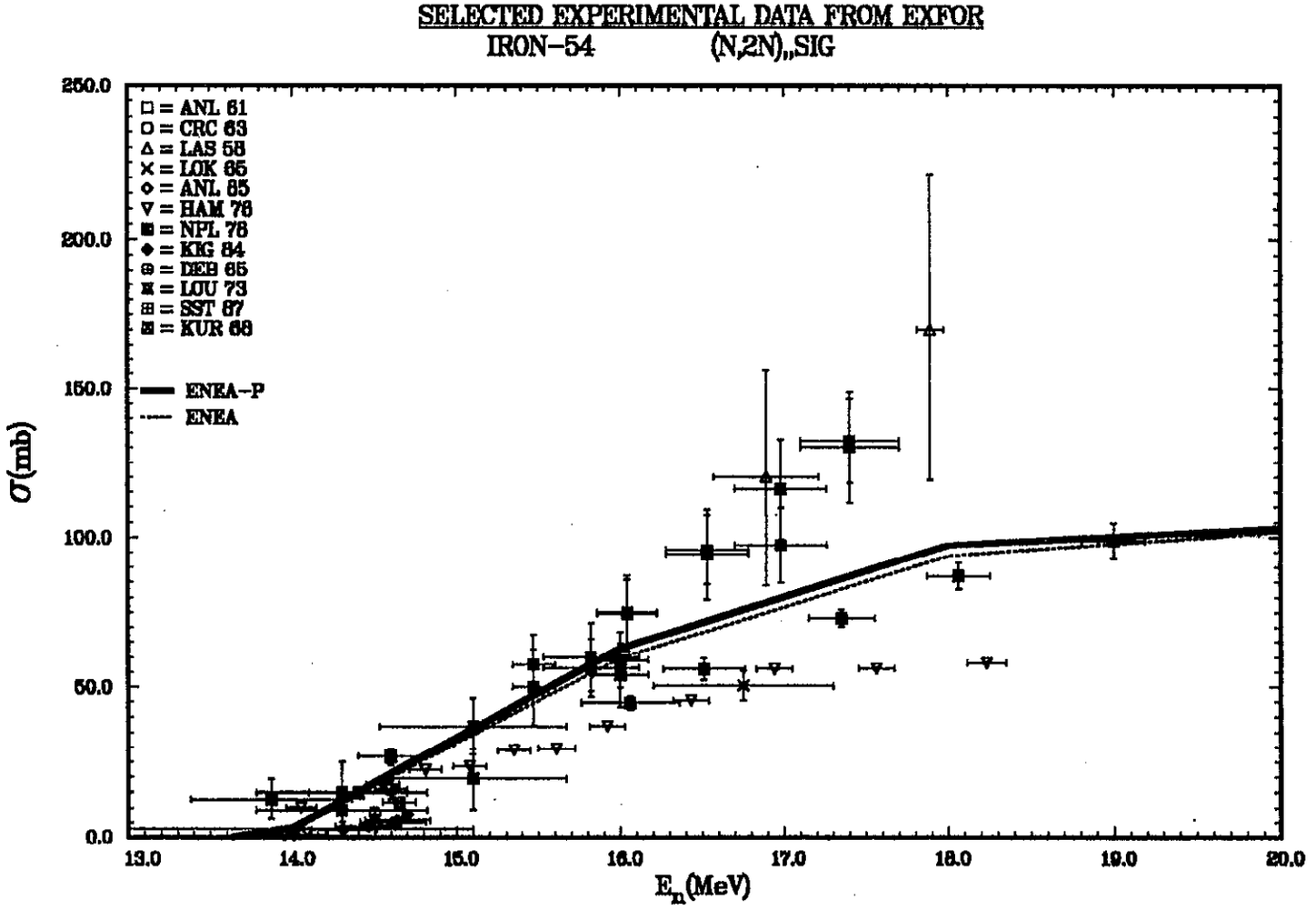

Fig. 3

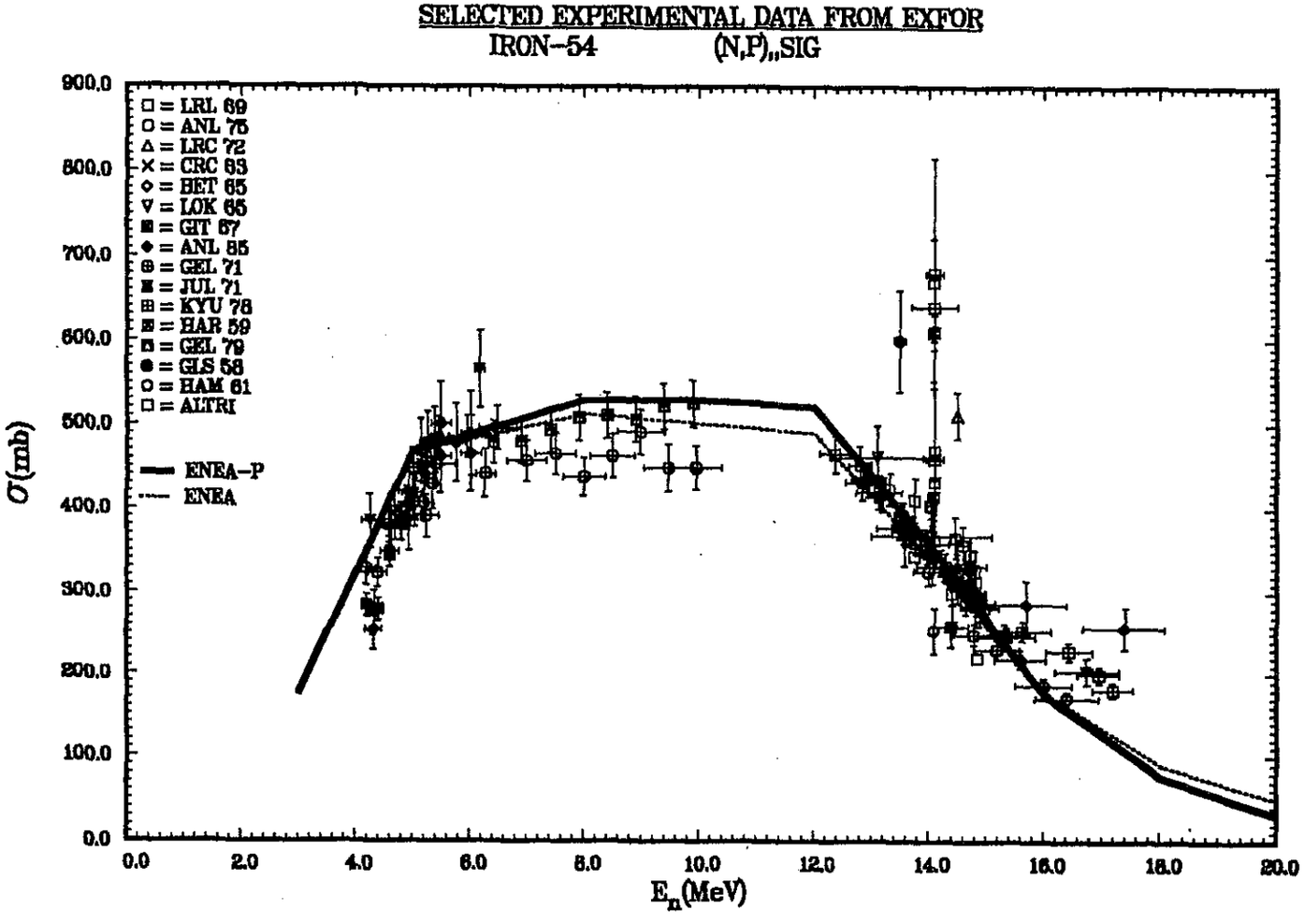

Fig. 4

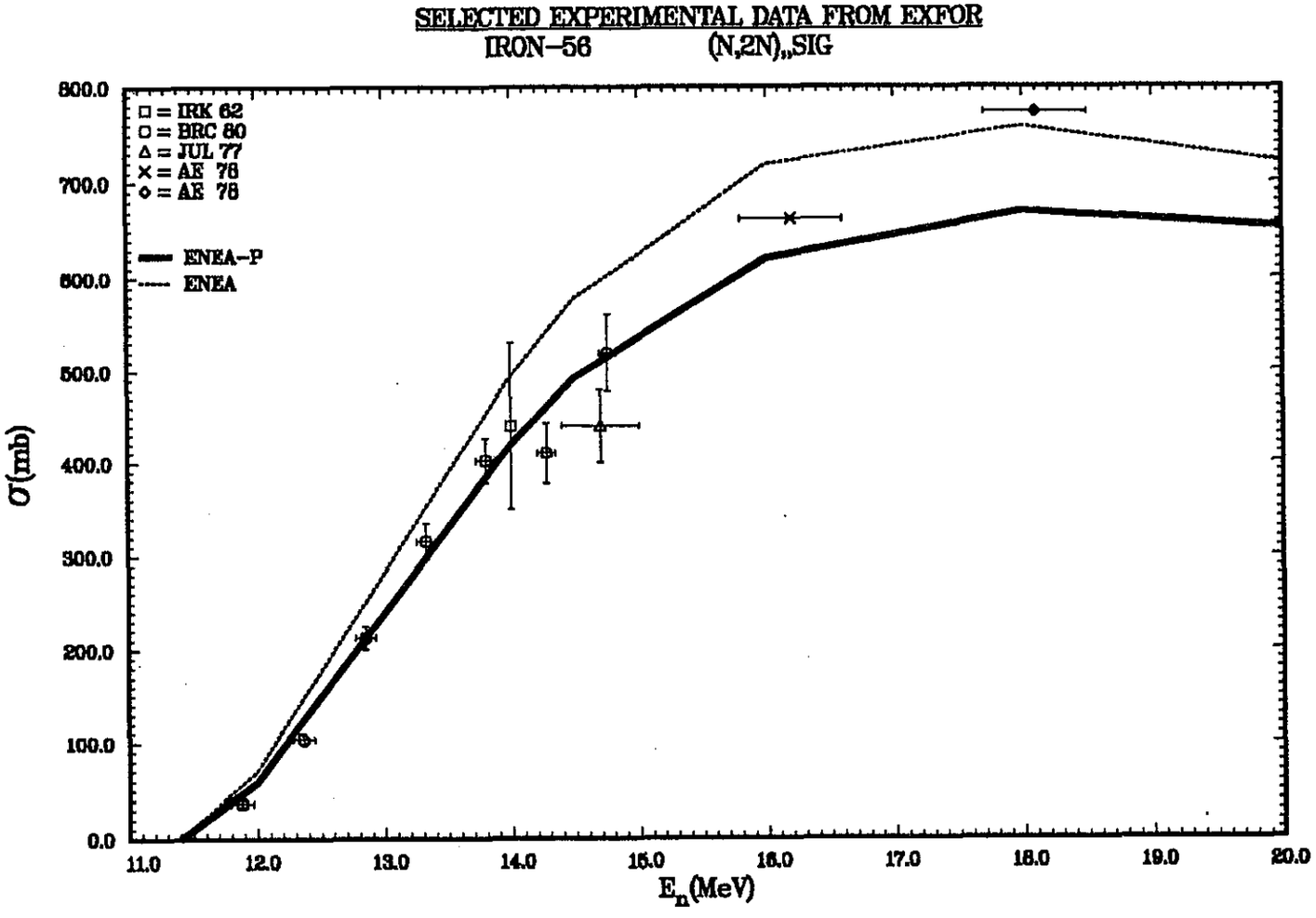

Fig. 5

Fig. 9

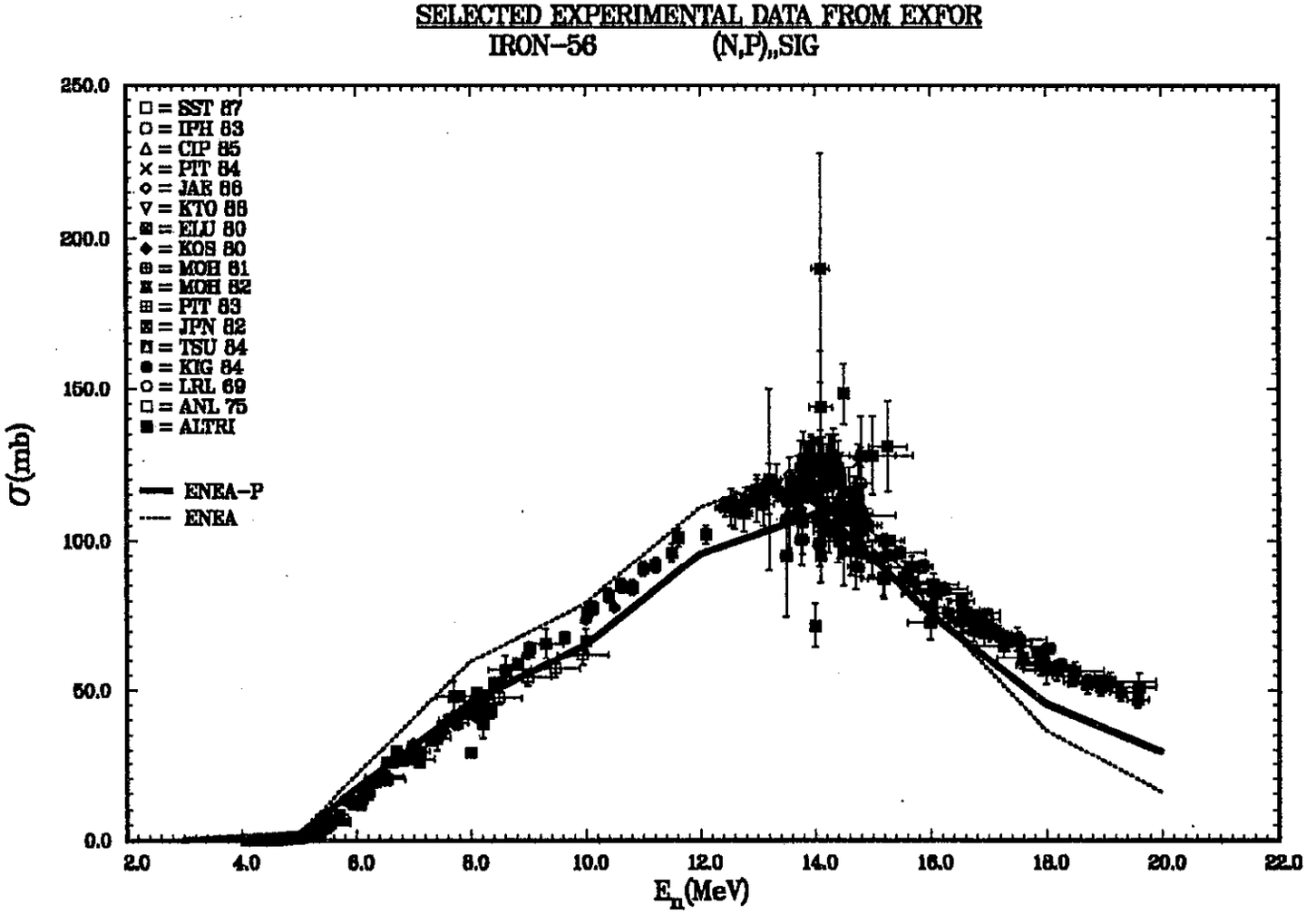

```
     FE 54  14.500 IB MAY 88
OPTICAL MODEL PARAMETERS USED ARE:
LA-N  FOR NEUTRON  NP-P FOR PROTON  DW-A FOR ALPHA
NDISP-  11  EPSI-  1.00E-08  NUMBER OF EXCITED GAMMA- 0
FE- 53  EOUT-   3.470  A-   8.250  UR-   1.000  SIGma2-   0.813
        M-  1.00  BETA-  0.00  E1+E2+M1
        E2-   34.00  GAMMA2-   8.00  SIGM2 -    0.004
        M1-    8.70  GAMMA1-   0.80  SIGM1 -    0.002
FE- 54  EOUT-   3.300  A-   8.250  UR-   1.000  SIGma2-   0.887
        M-  1.00  BETA-  0.00  E1+E2+M1
        E2-   34.00  GAMMA2-   8.00  SIGM2 -    0.004
        M1-    8.70  GAMMA1-   0.80  SIGM1 -    0.002
FE- 55  EOUT-   3.080  A-   8.728  UR-   1.000  SIGma2-   0.875
        M-  1.00  BETA-  0.00  E1+E2+M1
        E2-   34.00  GAMMA2-   8.00  SIGM2 -    0.004
        M1-    8.70  GAMMA1-   0.80  SIGM1 -    0.002
MN- 53  EOUT-   3.480  A-   8.250  UR-   1.000  SIGma2-   9.758
        M-  1.00  BETA-  0.00  E1+E2+M1
        M1-    0.00  GAMMA1-   0.00  SIGM1 -    0.000
N.NEXCNU-  2048  FMCT-   1.00
```

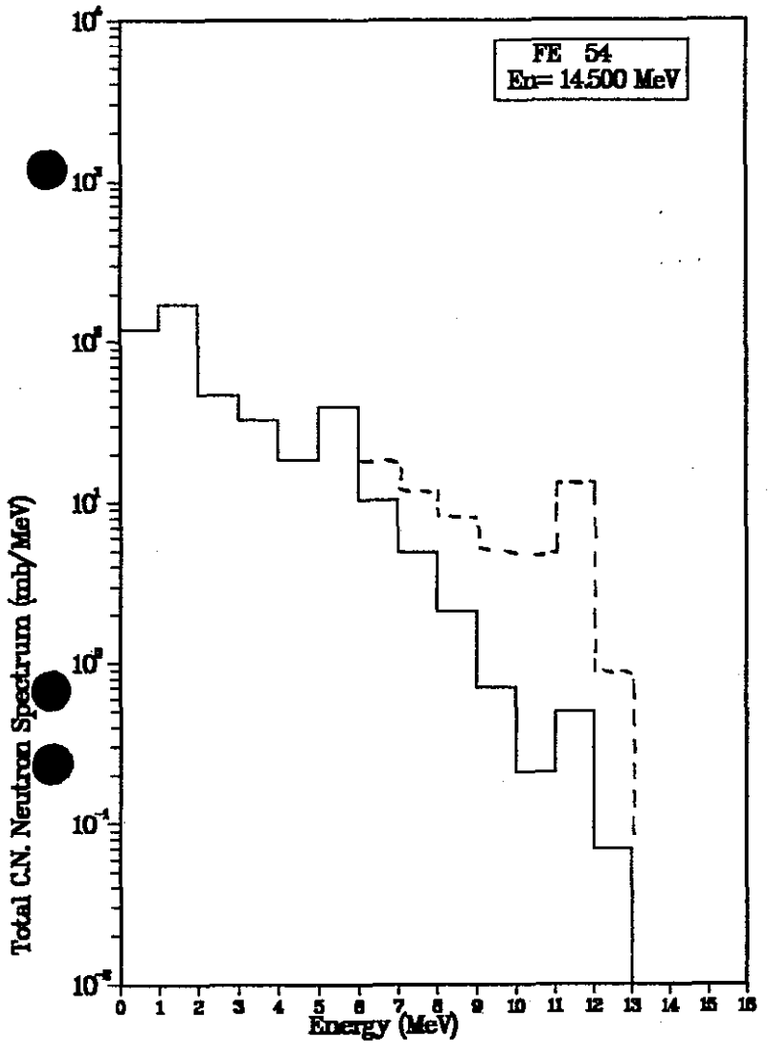

E (MEV)	I (BARNS/MEV)
0.00	0.1184
1.00	0.1737
2.00	0.0484
3.00	0.0550
4.00	0.0188
5.00	0.0085
6.00	0.0104
7.00	0.0048
8.00	0.0021
9.00	0.0007
10.00	0.0003
11.00	0.0003
12.00	0.0001
13.00	0.0000
TOTAL	0.4475

Fig. 7

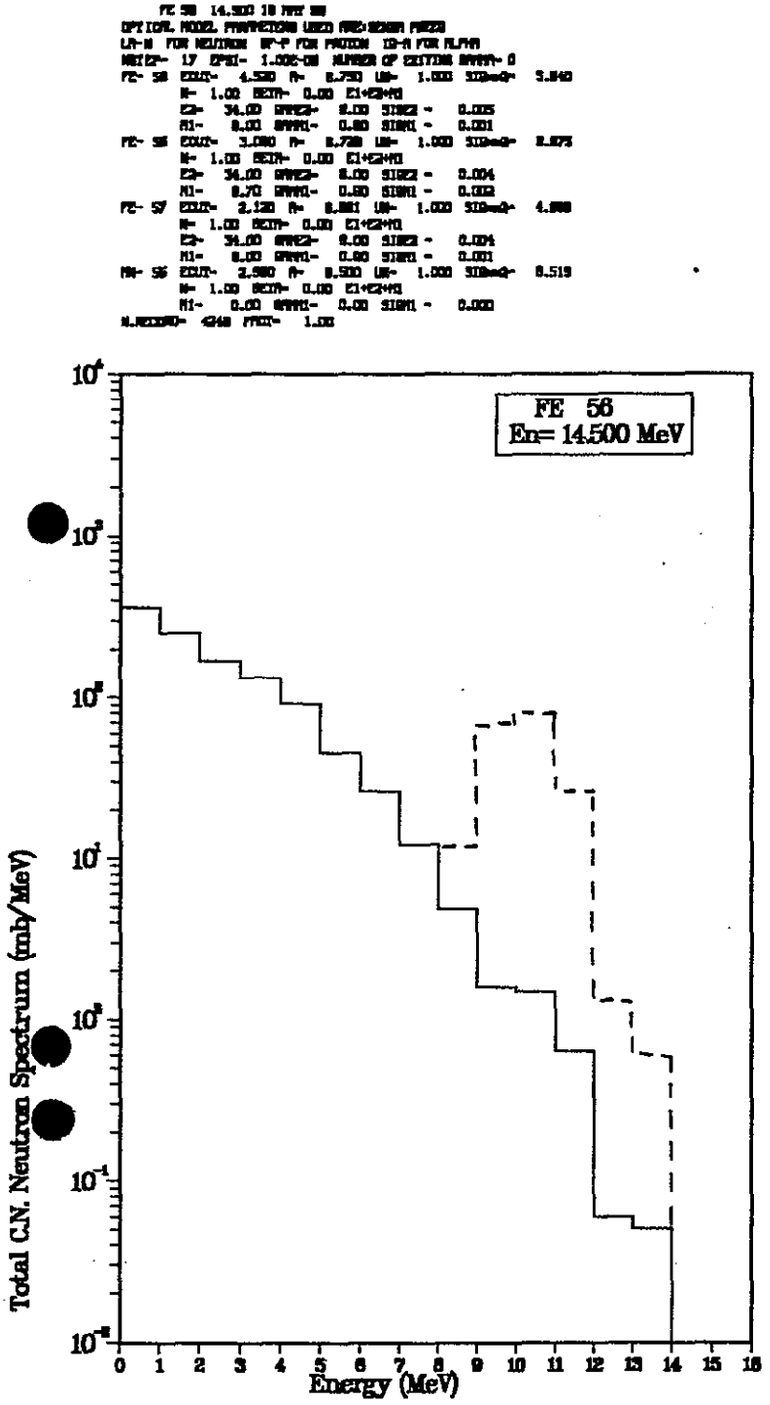

Fig. 8